Electronic Supplementary Material (ESI) for ChemComm.

Electronic supplementary information

Transformation from $[Au_{25}(SCH_2CH_2CH_2CH_3)_{18}]^0$ to $Au_{28}(SCH_2CH(CH_3)Ph)_{21}$ Gold Nanoclusters: Gentle Conditions is Enough

Yanan Wang, Belén Nieto-Ortega, Thomas Bürgi*

Department of Physical Chemistry, University of Geneva, 30 Quai Ernest-Ansermet, 1211 Geneva 4, Switzerland.

I. Supporting Tables

Table S1. Specific conditions of reported cluster transformatios induced by ligand exchange reactions.

Transformation		Ratio between $L_{incoming}/L_{outgoing}$	T(^{0}C)	Reaction time	reference
Larger → Smaller	$Au_{25}(PET)_{18} \rightarrow Au_{20}(TBBT)_{16}$	150:1	40^{0}C	8h	15
	$Au_{36}(SPhX)_{24} \rightarrow Au_{30}(S\text{-}tBu)_{18}$	800:1	80^{0}C	2h	16
	$Au_{38}(PET)_{24} \rightarrow Au_{36}(TBBT)_{24}$	160:1	80^{0}C	12h	14
	$Au_{144}(PET)_{60} \rightarrow Au_{99}(SPh)_{42}$	530:1	80^{0}C	3h	12
	$Au_{144}(PET)_{60} \rightarrow Au_{133}(TBBT)_{52}$	370:1	80^{0}C	4 h	13
Smaller → Larger	$Au_{25}(PET)_{18} \rightarrow Au_{28}(TBBT)_{20}$	120:1	80^{0}C	2h	17
	$Au_{30}(S\text{-}tBu)_{18} \rightarrow Au_{36}(SPhX)_{24}$	220:1	80^{0}C	16h	16
	$Au_{38}(SC_2H_4Ph)_{24} \rightarrow Au_{60}S_6(SCH_2Ph)_{36}$	180:1	100^{o}C	overnight	18
	$[Au_{23}(S\text{-}c\text{-}C_6H_{11})_{16}] \rightarrow [Au_{24}(SCH_2Ph\text{-}^tBu)_{20}]^0$	360:1	40^{0}C	36h	19

II. Experimental section

1. Synthesis and purification of $[Au_{25}(SBut)_{18}]^0$

12 equiv. of 1-butanethiol (1632 μl, 15.24 mmol) were added dropwise, under stirring and at room temperature, to a tetrahydrofuran (THF) solution (100 ml) of $HAuCl_4 \cdot 3H_2O$ (1 g, 2.54 mmol) and tetra-n-octylammonium bromide (1575 mg, 2.85 mmol). After 1 h, a freshly-prepared ice-cold solution of $NaBH_4$ (970 mg, 25.4 mmol) in milli-Q water (20 ml) was rapidly added under vigorous stirring. The resulting black mixture was stirred for ca. 3 days. Afterwards, the THF was removed by rotary evaporation to leave a red-brownish oil covered by an aqueous phase. The latter was removed by adding 200 mL of cold methanol and then filtered on paper. To remove excess thiol and other byproducts the product was washed with methanol, filtered and dissolved in dichloromethane (DCM) at least three times. Finally, the product was dried in a vacuum rotary evaporator at room temperature. By this procedure, the cluster is obtained as $[n\text{-}Oct_4N^+][Au_{25}(SBu)_{18}^-]$. The product was then further oxidized by

dissolution in dichloromethane (DCM, 5 ml) followed by passage through a silica gel column under aerobic conditions. The sample was stored at -18 °C. Characterization of the pure samples was carried out by UV-Vis spectroscopy and matrix-assisted laser desorption ionization time-of-flight (MALDI-TOF) mass spectrometry (Figures S1 and S2).

2. Synthesis and purification of $Au_{25}(PET)_{18}$

Similarly, to the synthesis of $[Au_{25}(SBut)_{18}]^0$ described above $[Au_{25}(PET)_{18}]^0$ was prepared by first synthesizing $Au_{25}(PET)_{18}^-$ (anion cluster) followed by oxidation by a silica gel column under aerobic conditions. Typically, $HAuCl_4 \cdot 3H_2O$ (1 g, 2.54 mmol) and TOAB (1.641 mg, 0.30 mmol) were combined in a 1 L round bottom flask, to which 250 mL THF solvent was added. After vigorous stirring for 15 min, the solution color changed from yellow to red. Then, C_8H_9SH (1.62 mL, 7.25 mmol) was slowly added to the flask at room temperature without changing the stirring speed. The solution color gradually changed from red to yellow and then to colorless within ~30 min. After that, an aqueous solution of $NaBH_4$ (0.918 g, 0.5 mmol, freshly dissolved in 50.0 mL of ice-cold mili-Q water) was added to the flask all at once. The reaction generated some bubbles and the solution turned black immediately, indicating the formation of Au nanoclusters. The reaction was allowed to proceed under constant stirring for ca. 2 days and eventually we obtained pure $Au_{25}(PET)_{18}^-$. After this point the purification and characterization followed the same procedure as described for $[Au_{25}(SBut)_{18}]^0$. Characterization of the pure samples was carried out by UV-Vis and MALDI-TOF mass spectrometry (Figures S3 and S4).

3. Characterization of $[Au_{25}(SBut)_{18}]^0$ and $[Au_{25}(PET)_{18}]^0$

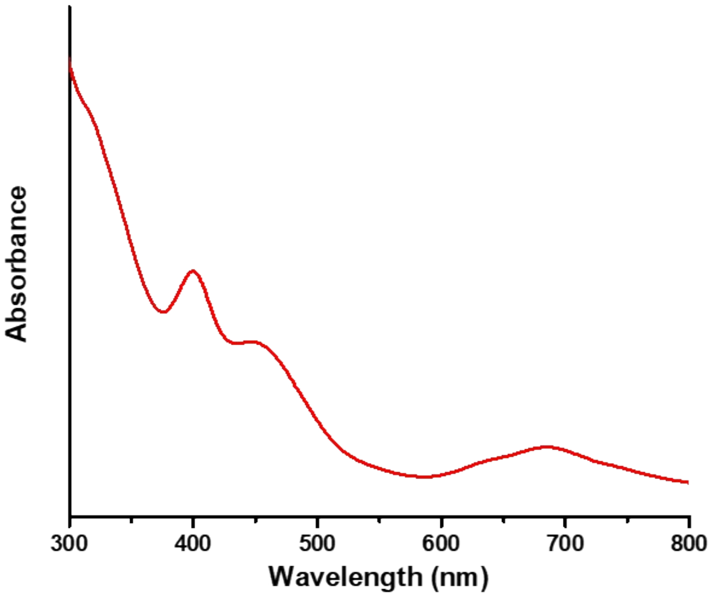

Figure S1. UV-vis absorption spectrum of $[Au_{25}(SBut)_{18}]^0$ in DCM. The spectrum was obtained using a quartz cuvette with a 2 mm optical-path length, at room temperature, and at 0.10 mM concentration.

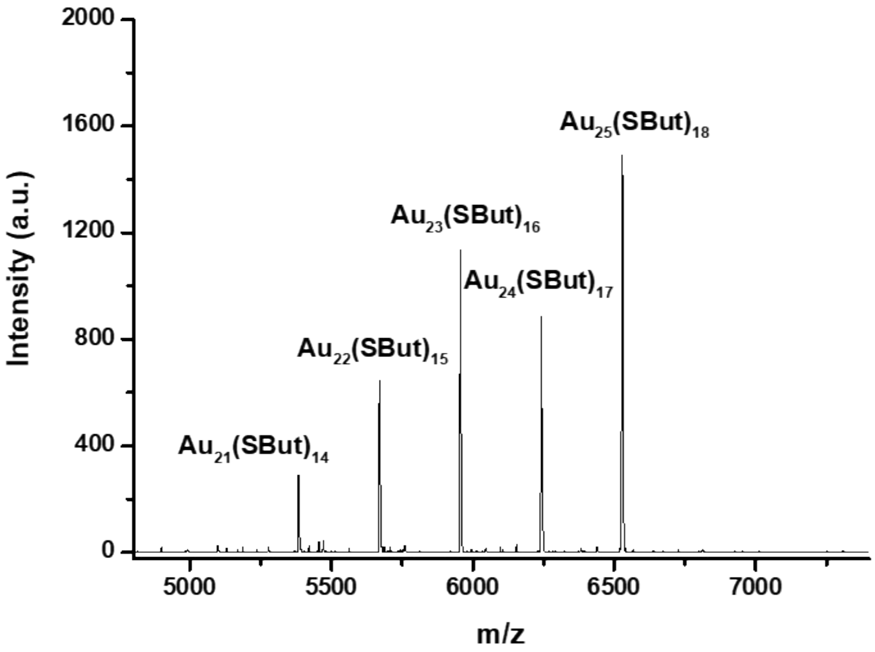

Figure S2. Positive-ion MALDI mass spectrum of $[Au_{25}(SBut)_{18}]^0$.

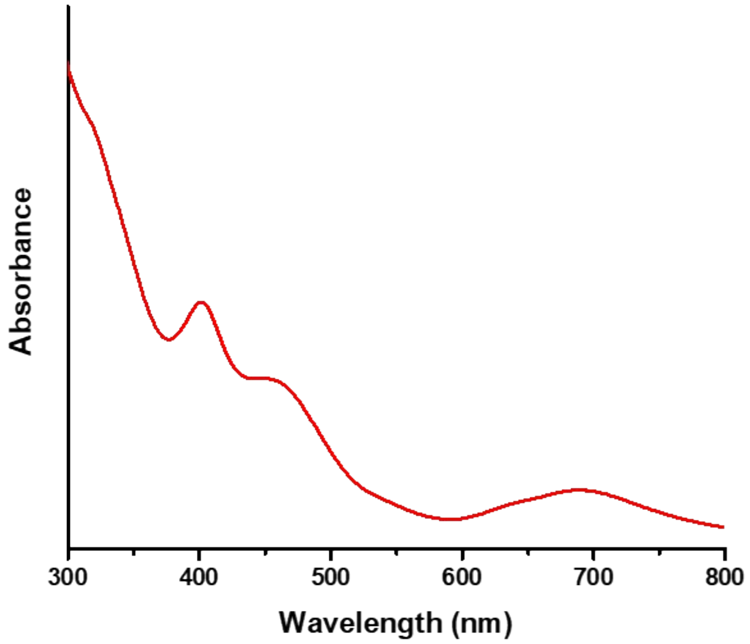

Figure S3. UV-vis absorption spectrum of $[Au_{25}(PET)_{18}]^0$ in DCM. The spectrum was obtained using a quartz cuvette with a 2 mm optical-path length, at room temperature, and at 0.10 mM concentration.

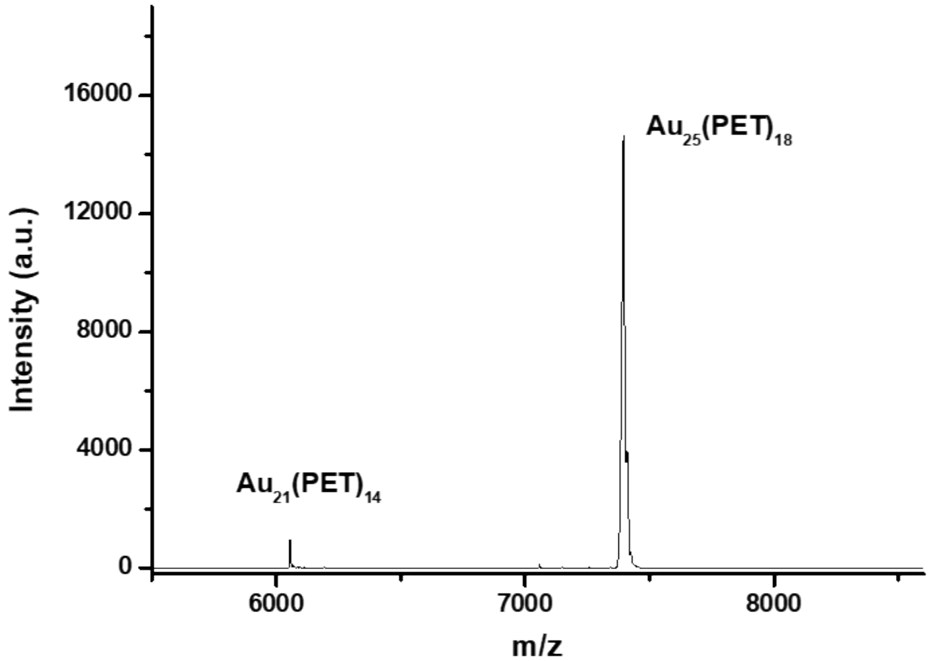

Figure S4. Positive-ion MALDI mass spectrum of $[Au_{25}(PET)_{18}]^0$.

4. Synthesis of R- and S-2-phenylpropane-1-thiol

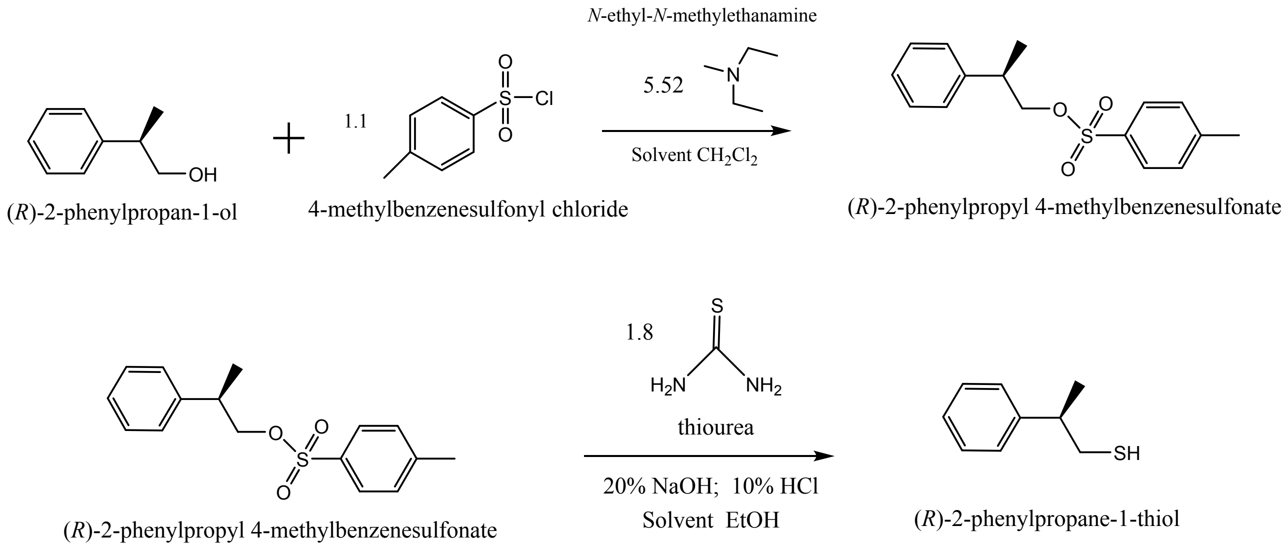

Scheme S1. Synthesis of (*R*)-2-phenylpropane-1-thiol

Synthesis of (*R*)-2-phenylpropane-1-thiol was performed according to the scheme above. The synthesis was adapted from ref [1]. With respect to this report the amount of thiourea was changed to 1.8 equivalents. (*S*)-2-phenylpropane-1-thiol was synthesized following the same protocol.

Racemic 2-phenylpropane-1-thiol was purchased from Enamine Ltd.

III. Ligand exchange reactions

$[Au_{25}(SBut)_{18}]^0$ + 2 equivalents of S-PPT

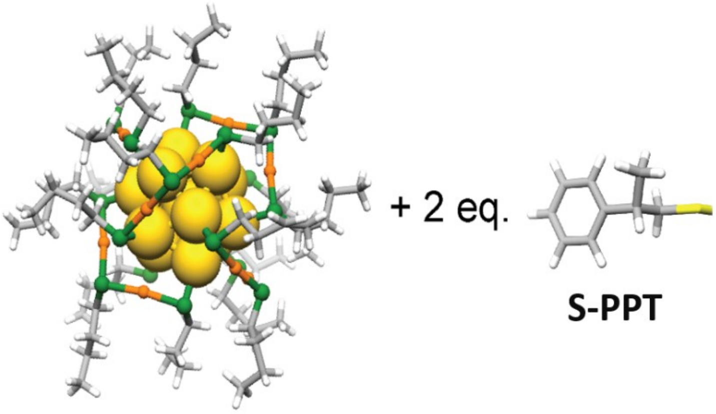

Table S2: Experimental conditions

	$[Au_{25}(SBut)_{18}]^0$	*S-PPT*
MW (g/mol)	6529.40	151.25
mg	10	8.339
mmol	1.532×10^{-3}	5.514×10^{-2}
mmol in thiol	2.757×10^{-2}	5.514×10^{-2}
Equivalents in thiol	1	2

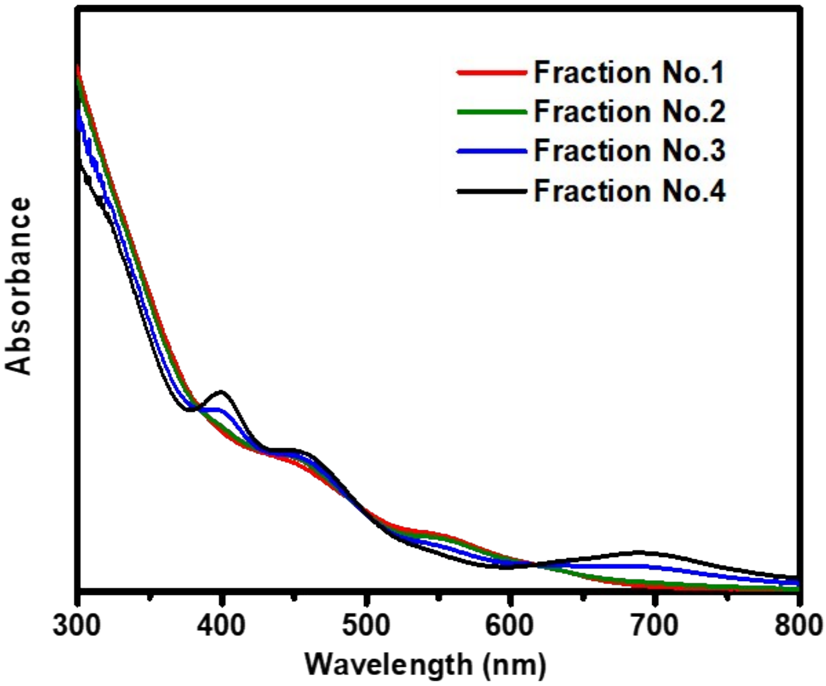

Figure S5. UV-Vis spectra of fractions obtained after LER of 0.1 mM of $[Au_{25}(SBut)_{18}]^0$ with S-PPT at room temperature in dichloromethane. The SBut:S-PPT ratio is 1:2.

$[Au_{25}(SBut)_{18}]^0$ + 2 equivalents of R-PPT

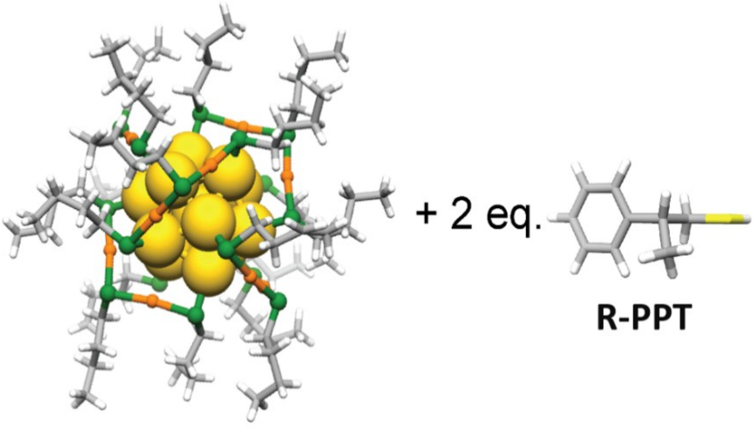

Table S3: Experimental conditions

	$[Au_{25}(SBut)_{18}]^0$	*R-PPT*
MW (g/mol)	6529.40	151.25
mg	10	8.339
mmol	1.532×10^{-3}	5.514×10^{-2}
mmol in thiol	2.757×10^{-2}	5.514×10^{-2}
Equivalents in thiol	1	2

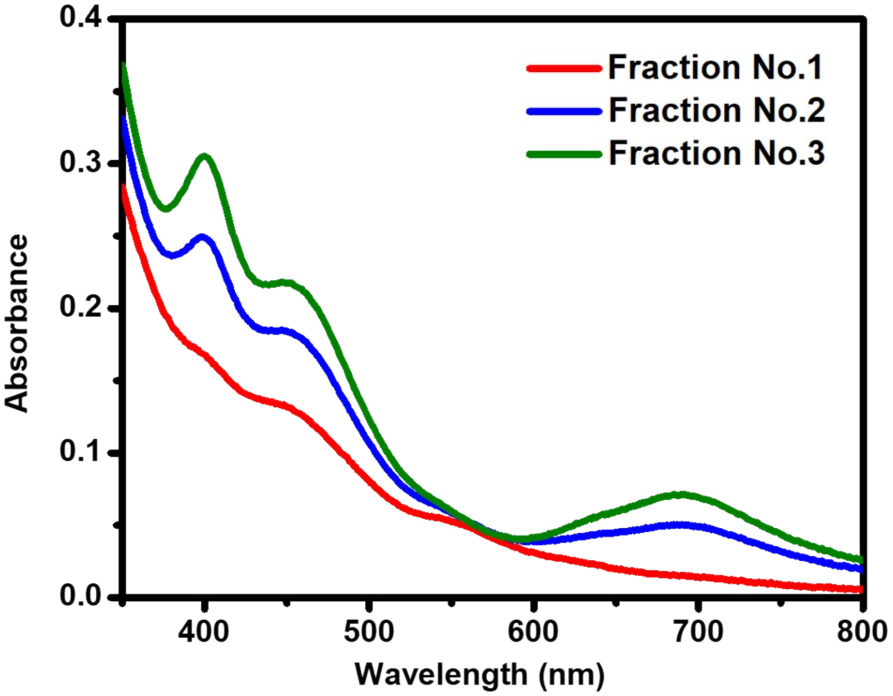

Figure S6. UV-Vis spectra of fractions obtained after LER of 0.1 mM of $[Au_{25}(SBut)_{18}]^0$ with R-PPT at room temperature in dichloromethane. The SBut:R-PPT ratio is 1:2.

$[Au_{25}(SBut)_{18}]^0$ + 1 equivalents of R-PPT

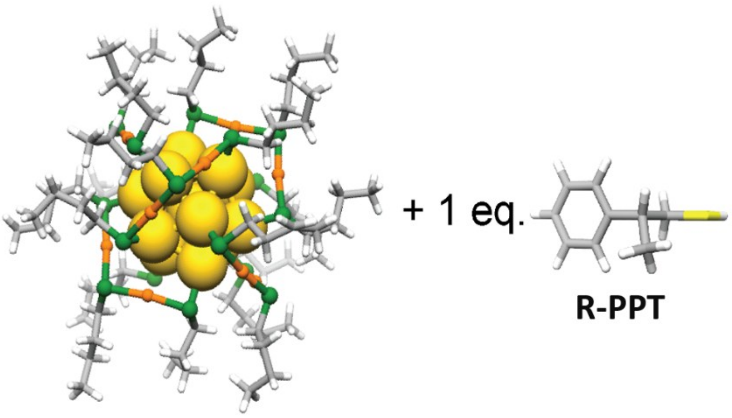

Table S4: Experimental conditions

	$[Au_{25}(SBut)_{18}]^0$	*R-PPT*
MW (g/mol)	6529.40	151.25
mg	10	4.1696
mmol	$1.532x10^{-3}$	$2.757x10^{-2}$
mmol in thiol	$2.757x10^{-2}$	$2.757x10^{-2}$
Equivalents in thiol	1	1

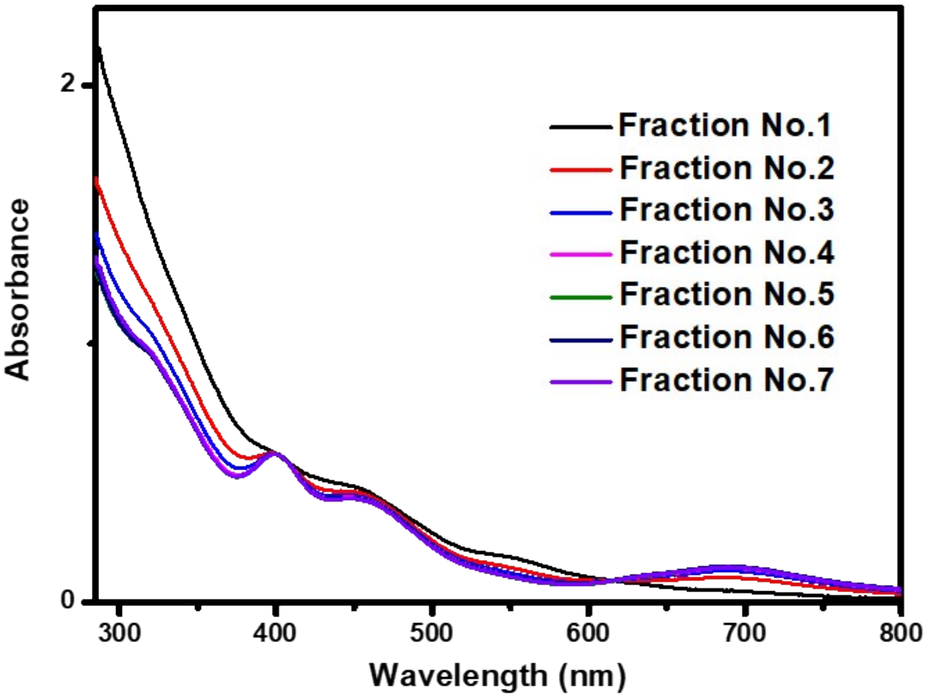

Figure S7. UV-Vis spectra of fractions obtained after LER of 0.1 mM of $[Au_{25}(SBut)_{18}]^0$ with R-PPT at room temperature in dichloromethane. The SBut:R-PPT ratio is 1:1.

$[Au_{25}(SBut)_{18}]^0$ + 5 equivalents of R-PPT

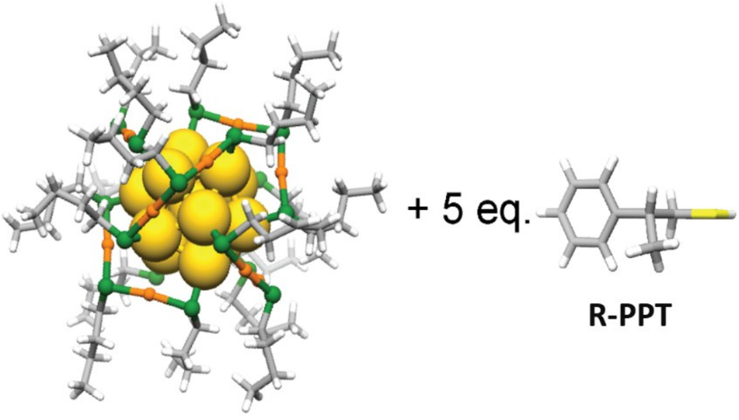

Table S5: Experimental conditions

	$[Au_{25}(SBut)_{18}]^0$	*R-PPT*
MW (g/mol)	6529.40	151.25
mg	10	20.848
mmol	1.532×10^{-3}	0.1378
mmol in thiol	2.757×10^{-2}	0.1378
Equivalents in thiol	1	5

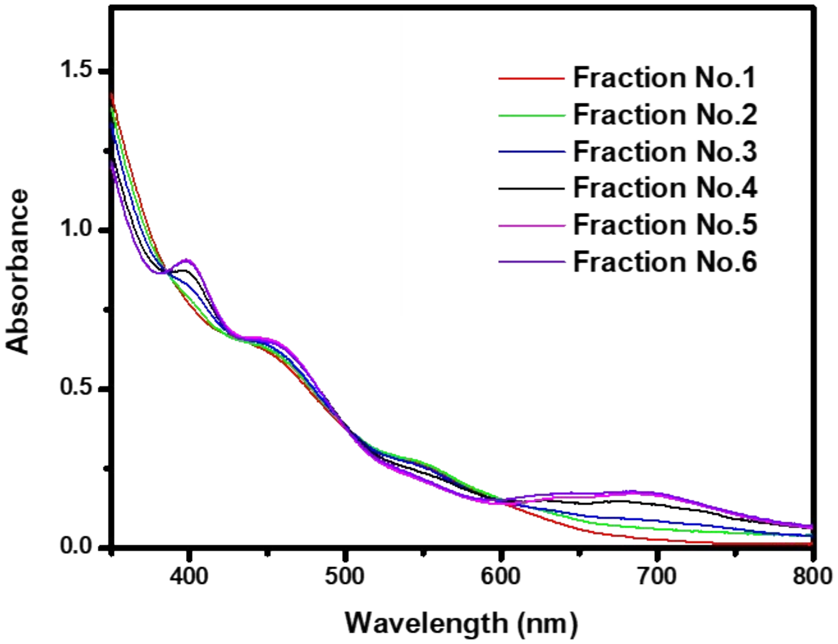

Figure S8. UV-Vis spectra of fractions obtained after LER of 0.1 mM of $[Au_{25}(SBut)_{18}]^0$ with R-PPT at room temperature in dichloromethane. The SBut:R-PPT ratio is 1:5.

.

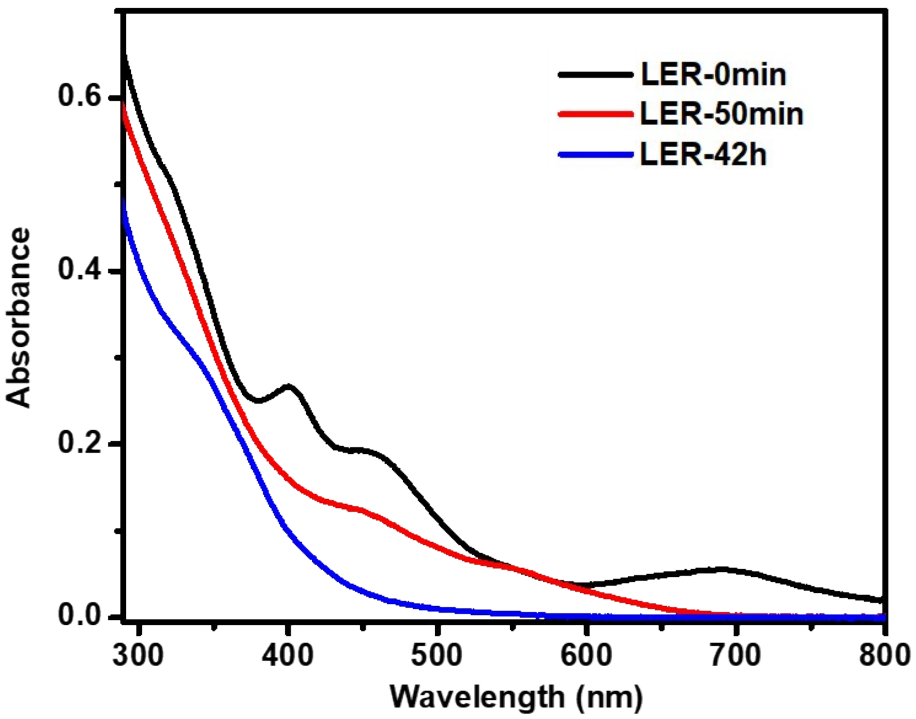

Figure S9. Time-resolved UV-Vis spectra of LER between $[Au_{25}(SBut)_{18}]^0$ and excess R-PPT in ratio SBut:R-PPT=1:5. Spectra were recorded at time 0, 1 and 42 hours. After 42 hours the spectrum becomes featureless and above 400 nm no peaks can be found.

$[Au_{25}(PET)_{18}]^0$ + 2 equivalents of R-PPT

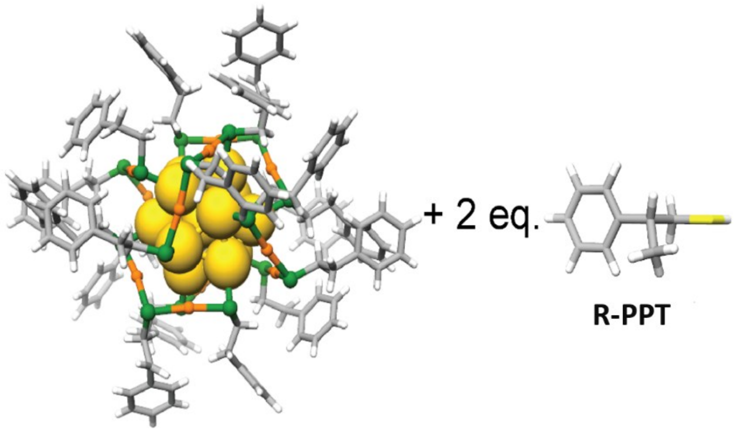

Table S6: Experimental conditions

	$[Au_{25}(PET)_{18}]^0$	R-PPT
MW (g/mol)	7394.30	151.25
mg	10	7.364
mmol	1.352×10^{-3}	4.869×10^{-2}
mmol in thiol	2.434×10^{-2}	4.869×10^{-2}
Equivalents in thiol	1	2

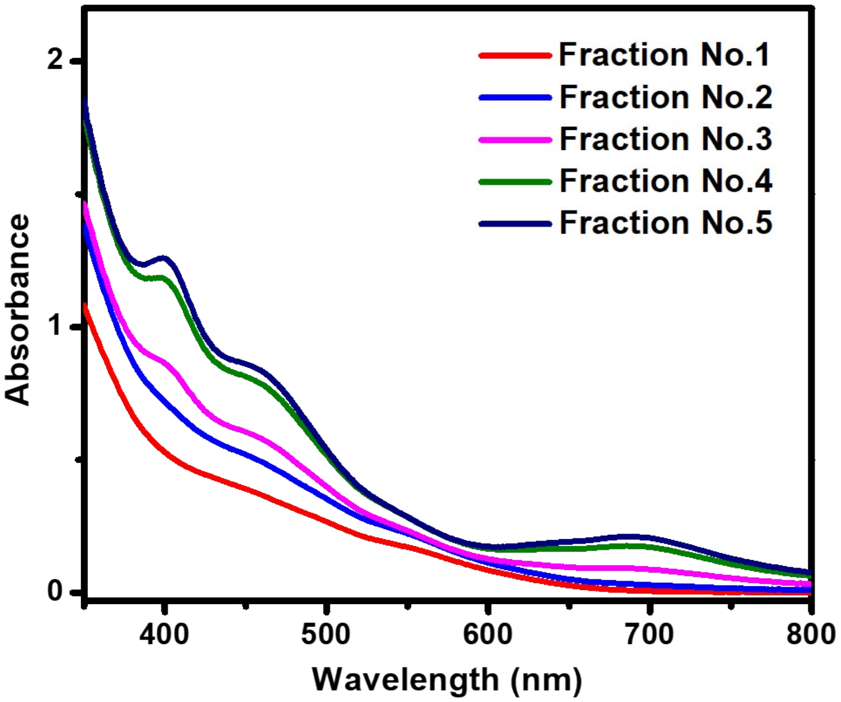

Figure S10. UV-Vis spectra of fractions obtained after LER of 0.1 mM of $[Au_{25}(PET)_{18}]^0$ with R-PPT. The PET:R-PPT ratio is 1:2.

$Au_{28}(S\text{-}PPT)_{21}$ + 2 equivalents of SBut

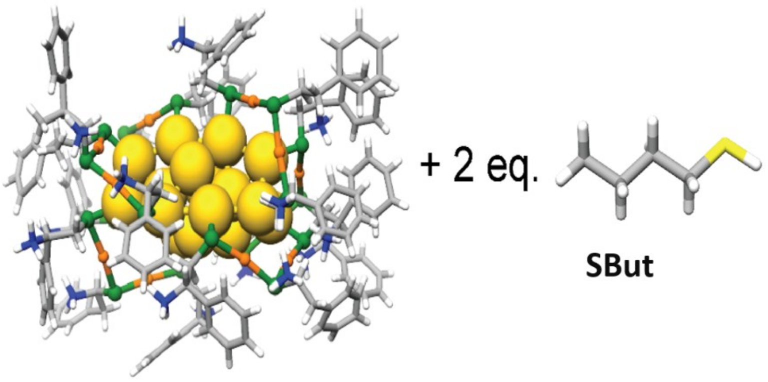

Table S7: Experimental conditions

	$Au_{28}(S\text{-}PPT)_{21}$	*SBut*
MW (g/mol)	8691.0	90.19
mg	10	4.358
mmol	$1.151\text{x}10^{-3}$	$4.832\text{x}10^{-2}$
mmol in thiol	$2.416\text{x}10^{-2}$	$4.832\text{x}10^{-2}$
Equivalents in thiol	1	2

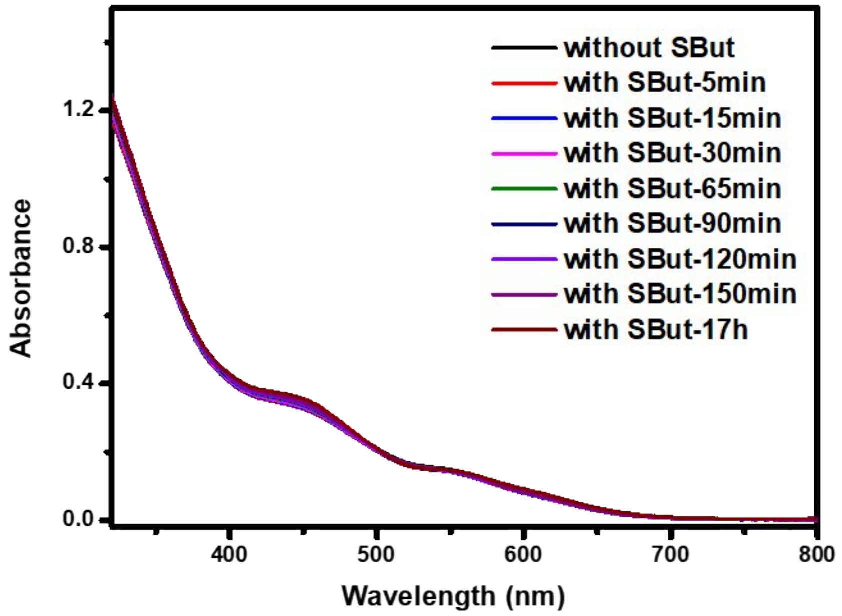

Figure S11. UV-Vis spectra of LER between $Au_{28}(S\text{-}PPT)_{21}$ and SBut**.**

$[Au_{25}(PET)_{18}]^0$ + 2 equivalents of SBut

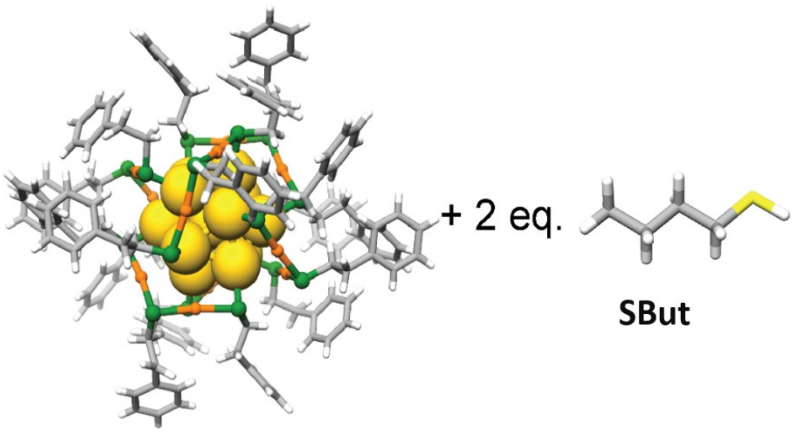

Table S8: Experimental conditions

	$[Au_{25}(PET)_{18}]^0$	*SBut*
MW (g/mol)	7394.30	90.19
mg	10	4.391
mmol	1.352×10^{-3}	4.869×10^{-2}
mmol in thiol	2.434×10^{-2}	4.869×10^{-2}
Equivalents in thiol	1	2

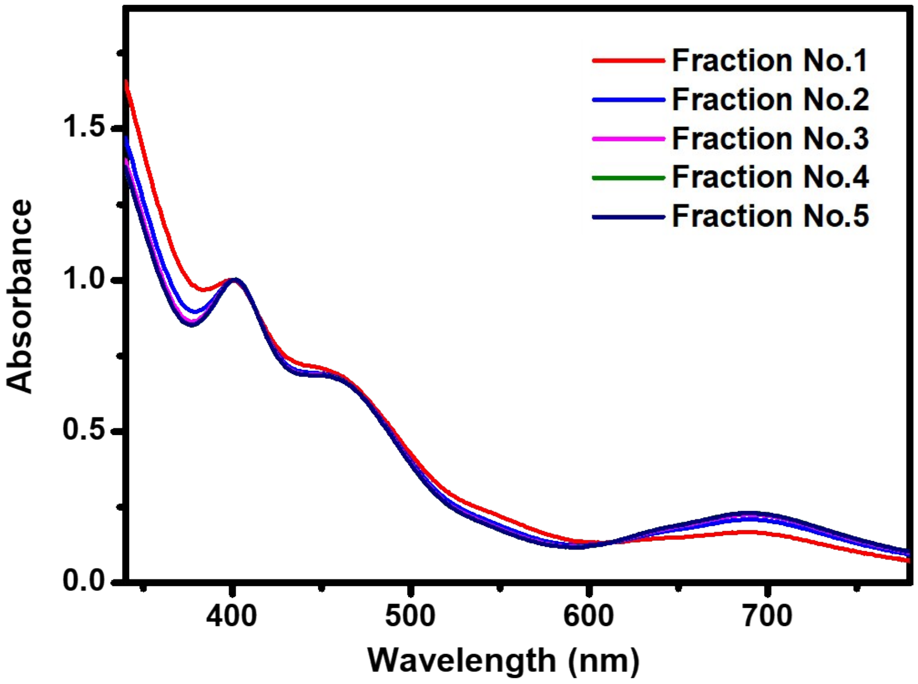

Figure S12. UV-Vis spectra of fractions obtained after LER of 0.1 mM of $[Au_{25}(PET)_{18}]^0$ with SBut. The PET:SBut is 1:2.

$\underline{[Au_{25}(SBut)_{18}]^0 \text{ + 2 equivalents of PET}}$

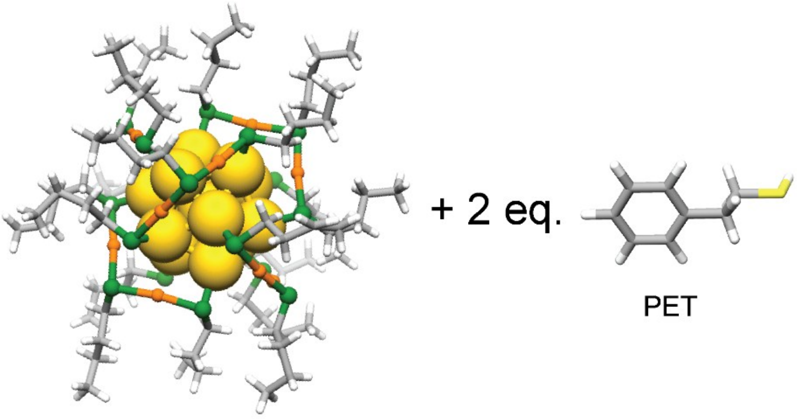

Table S9: Experimental conditions

	$[Au_{25}(SBut)_{18}]^0$	*PET*
MW (g/mol)	6529.40	138.23
mg	10	7.621
mmol	1.532×10^{-3}	5.514×10^{-2}
mmol in thiol	2.757×10^{-2}	5.514×10^{-2}
Equivalents in thiol	1	2

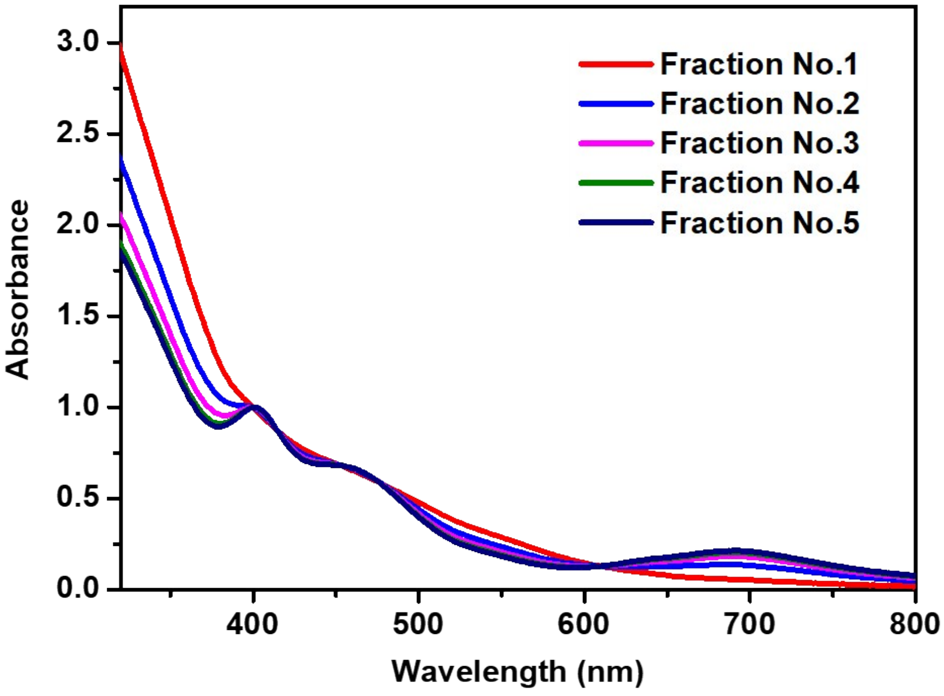

Figure S13. UV-Vis spectra of fractions obtained after LER of 0.1 mM of $[Au_{25}(SBut)_{18}]^0$ with PET.

$[Au_{25}(SBut)_{18}]^0$ + 2 equivalents of *rac*-PPT

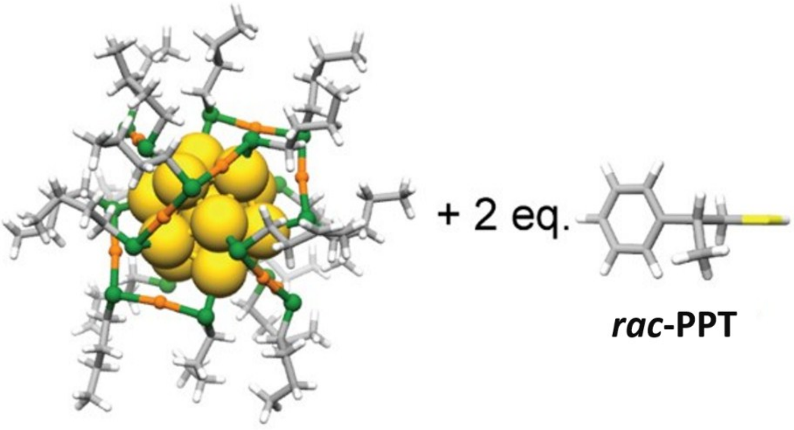

Table S10: Experimental conditions

	$[Au_{25}(SBut)_{18}]^0$	*Rac-PPT*
MW (g/mol)	6529.40	151.25
mg	10	8.339
mmol	1.532×10^{-3}	5.514×10^{-2}
mmol in thiol	2.757×10^{-2}	5.514×10^{-2}
Equivalents in thiol	1	2

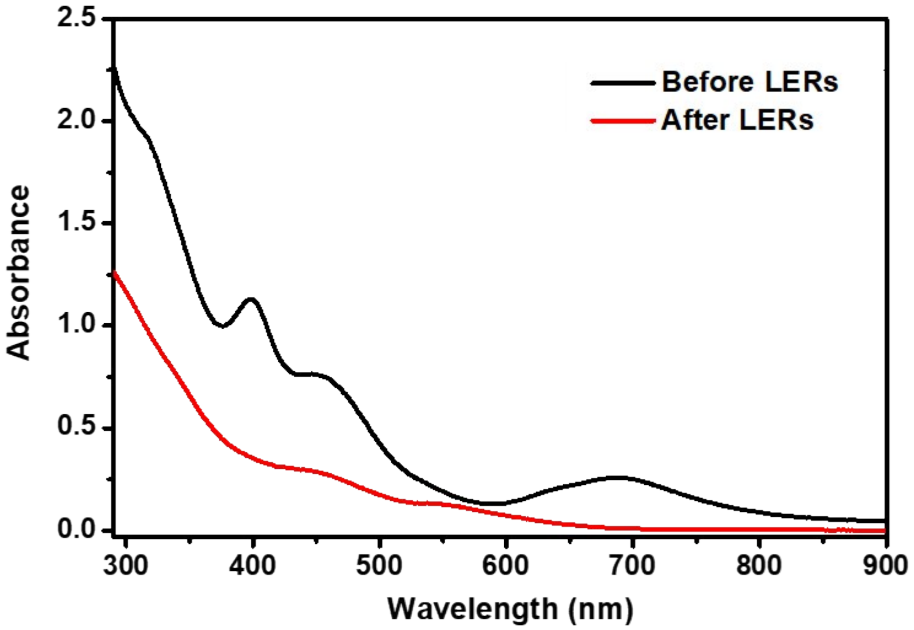

Figure S14. UV-Vis spectra of fractions obtained after LER of 0.1 mM of $[Au_{25}(SBut)_{18}]^0$ with *Rac*-PPT at room temperature in dichloromethane. The SBut:*Rac*-PPT ratio is 1:2.

IV. Nuclear magnetic resonance spectroscopy (NMR)

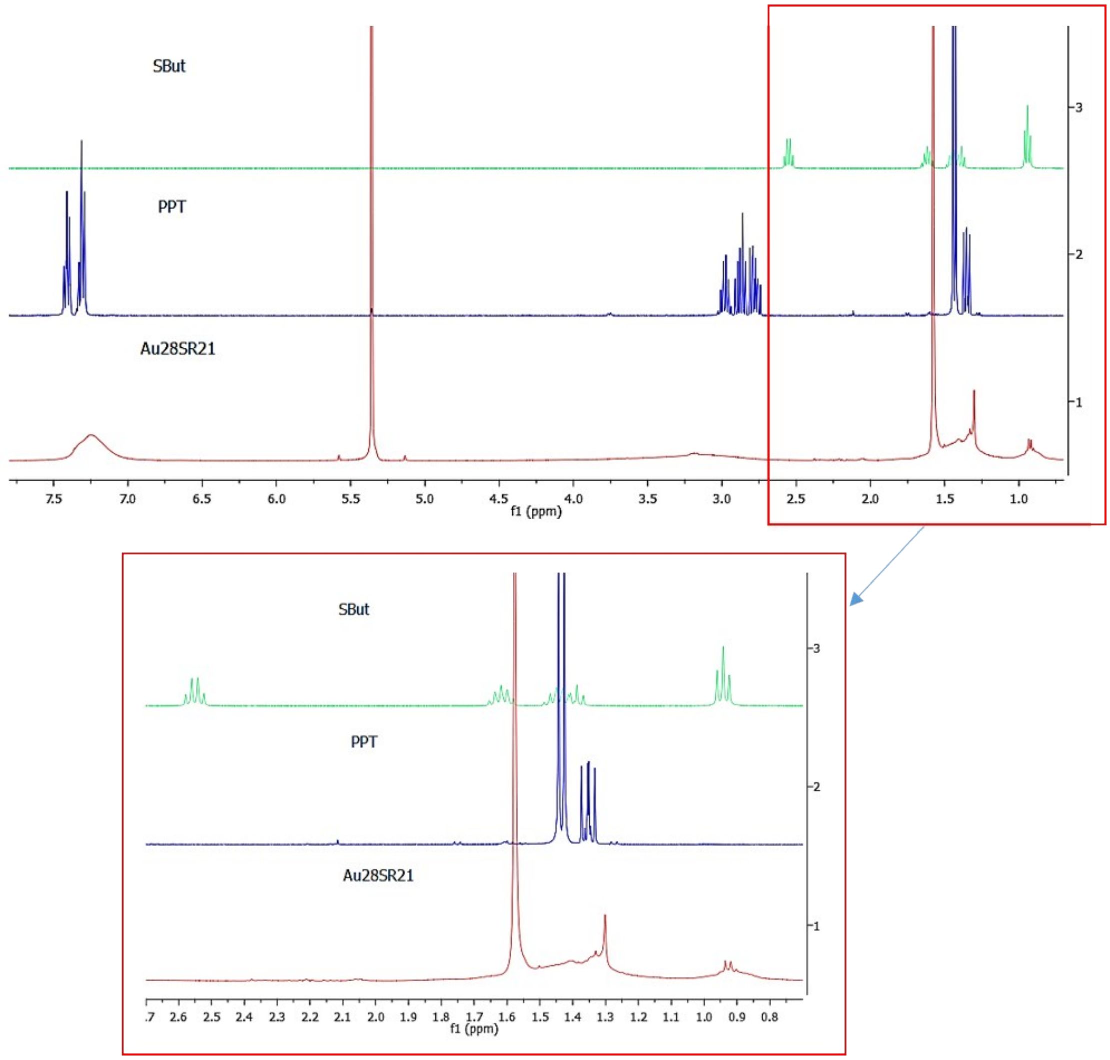

Figure S15. ^{1}H-NMR spectra of $Au_{28}SR_{21}$ cluster (red curve), SBut ligand (blue curve) and PPT ligand (green curve). All the spectra were recorded in deuterated DCM.

V. **Electrospray ionization (ESI) mass spectroscopy**

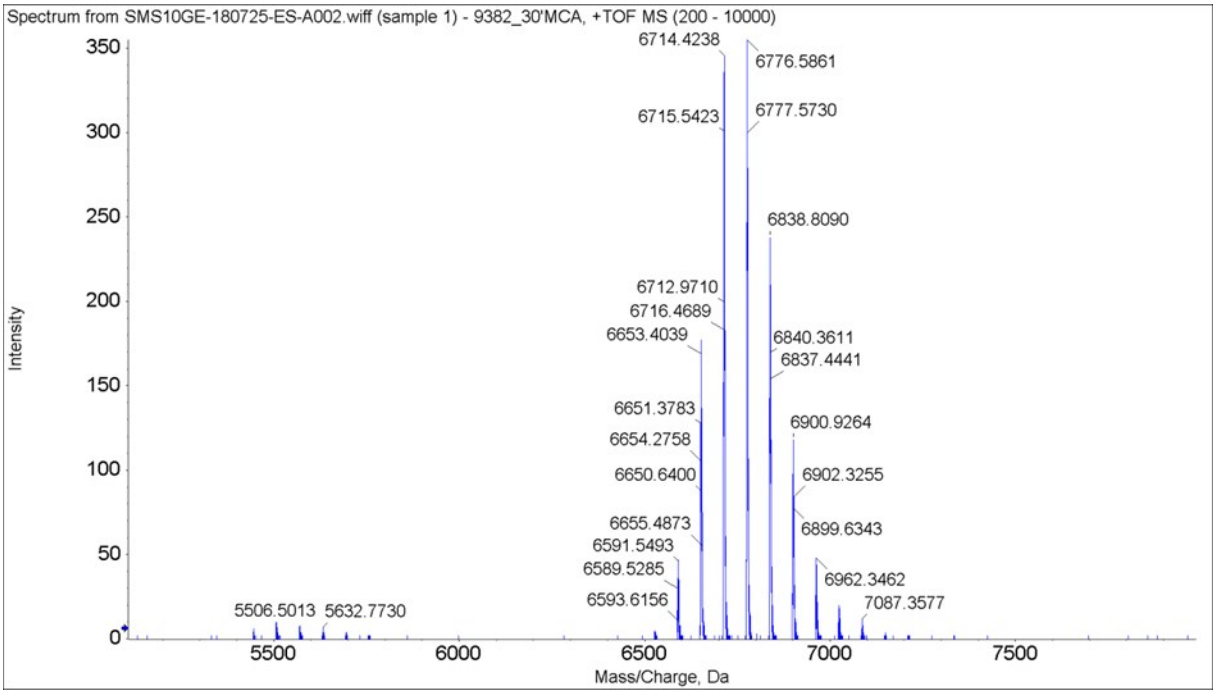

Figure S16. Electrospray ionization (ESI) mass spectroscopy in positive mode of the fraction 2 from Figure 1.

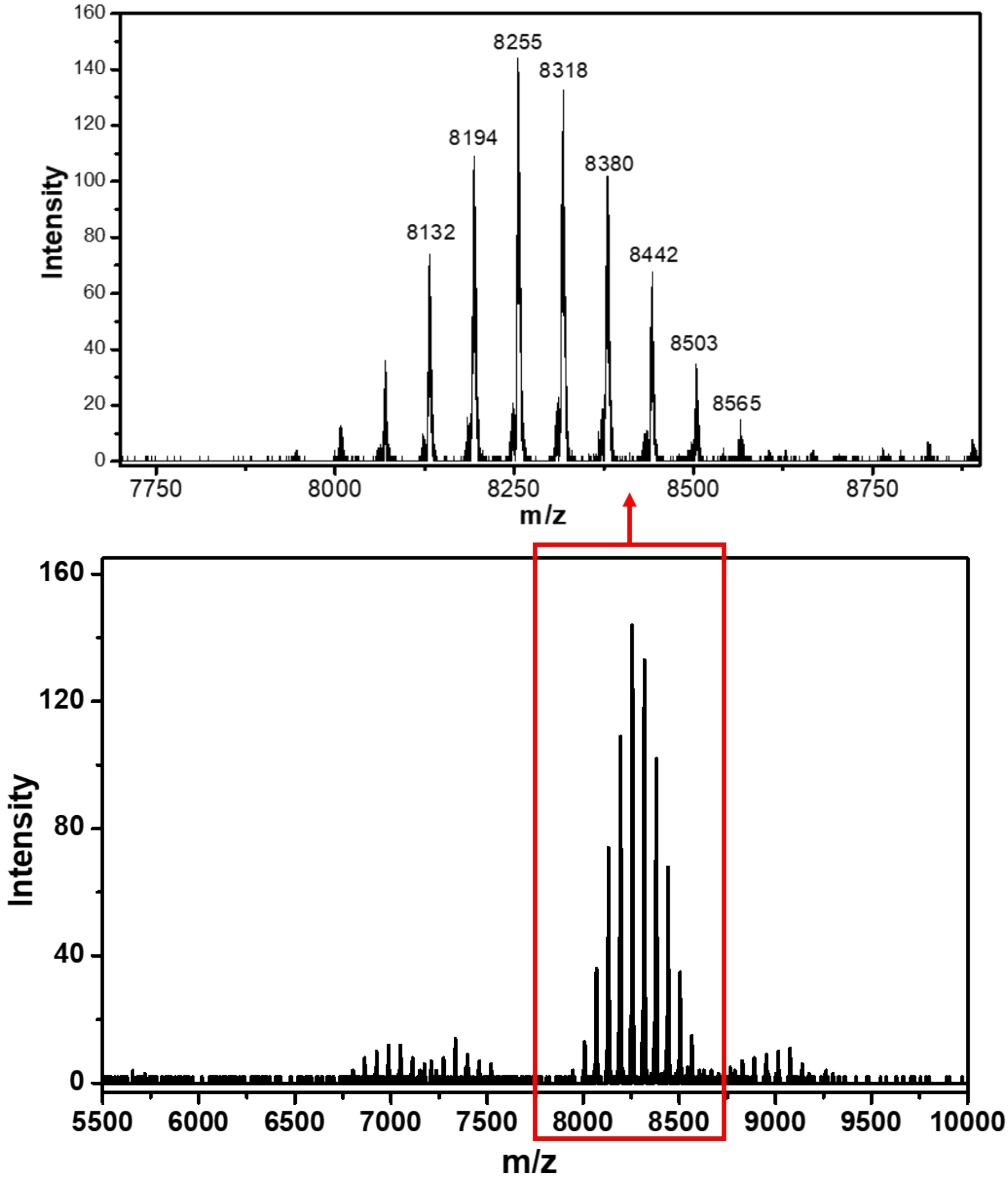

Figure S17. Electrospray ionization (ESI) mass spectroscopy in positive mode of the fraction 1 from Figure 1.

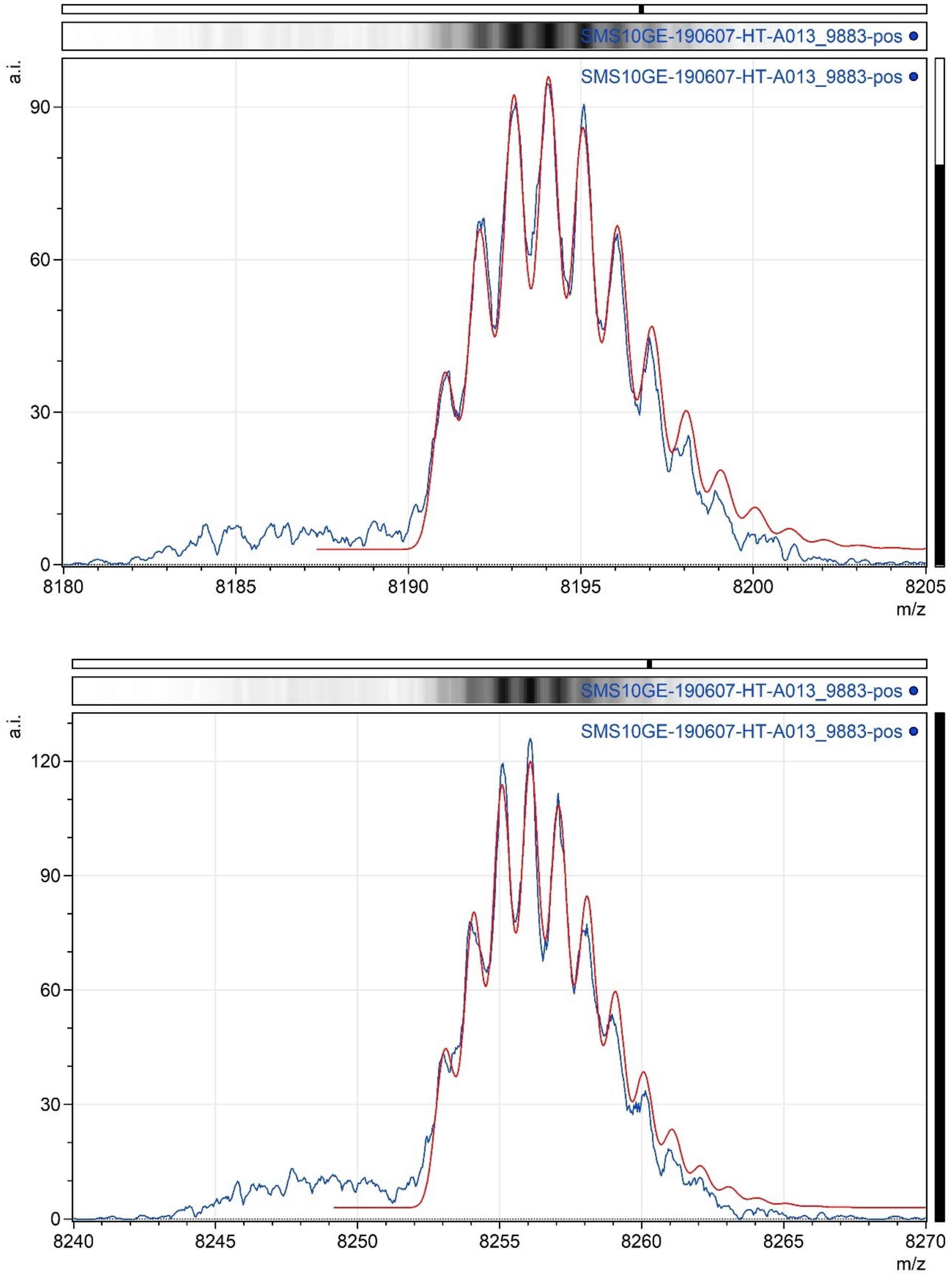

Figure S18. Experimental isotopic peaks (blue curve) and calculated isotopic pattern (red curve, using mMass) Fitting conditions: shape (symmetrical), FWHM (0.78), Intensity (100), baseline (3), shift (-0.1). Elemental formula used for calculation fitting: $Au_{28}S_{21}C_{149}H_{215}$ (top, corresponding to $Au_{28}(SBut)_8(S\text{-}PPT)_{13}$) and $Au_{28}S_{21}C_{154}H_{217}$ (bottom, equal to $Au_{28}(SBut)_7(S\text{-}PPT)_{14}$).

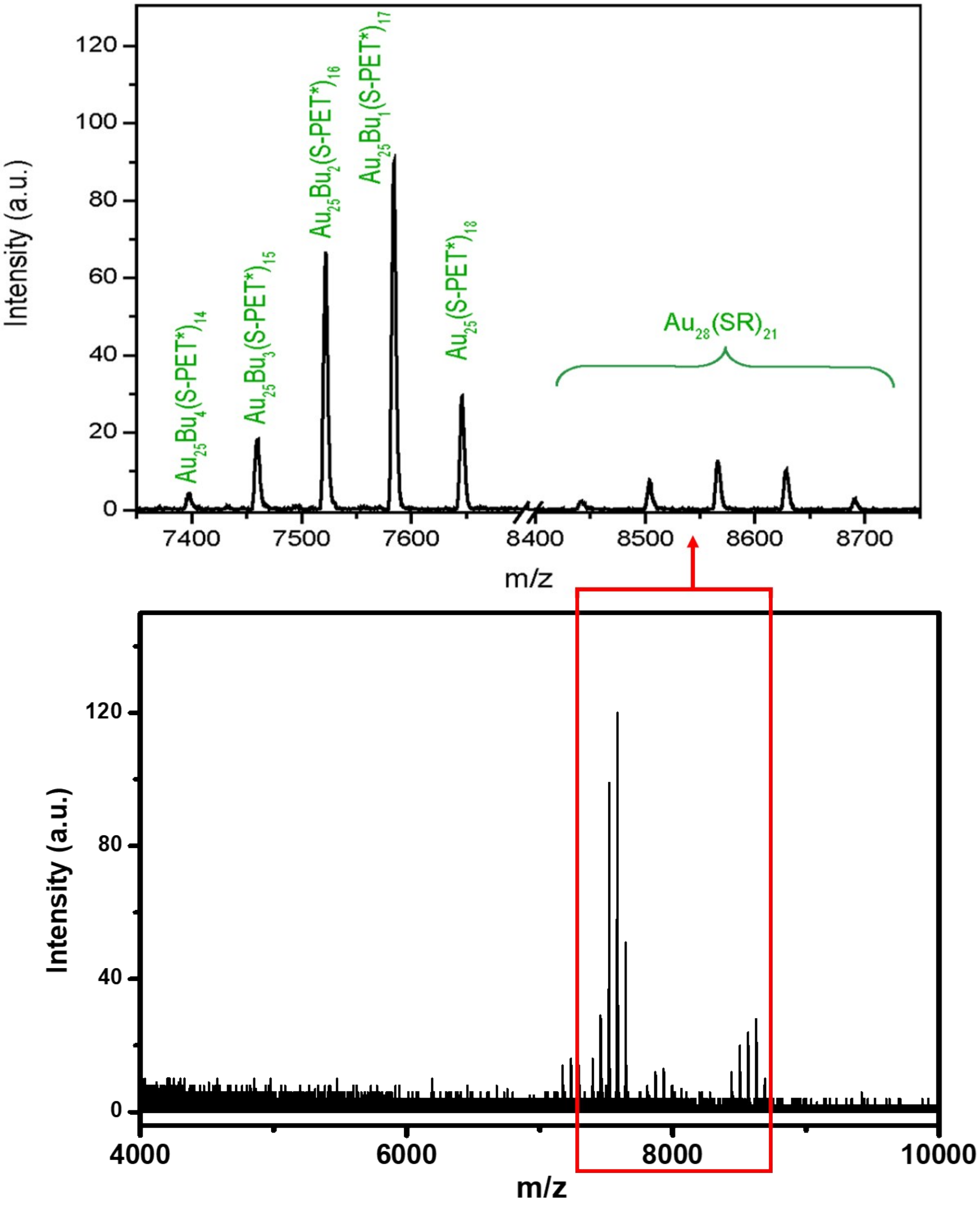

Figure S19. Electrospray ionization (ESI) mass spectroscopy in positive mode of the fraction 1 from Figure 1.

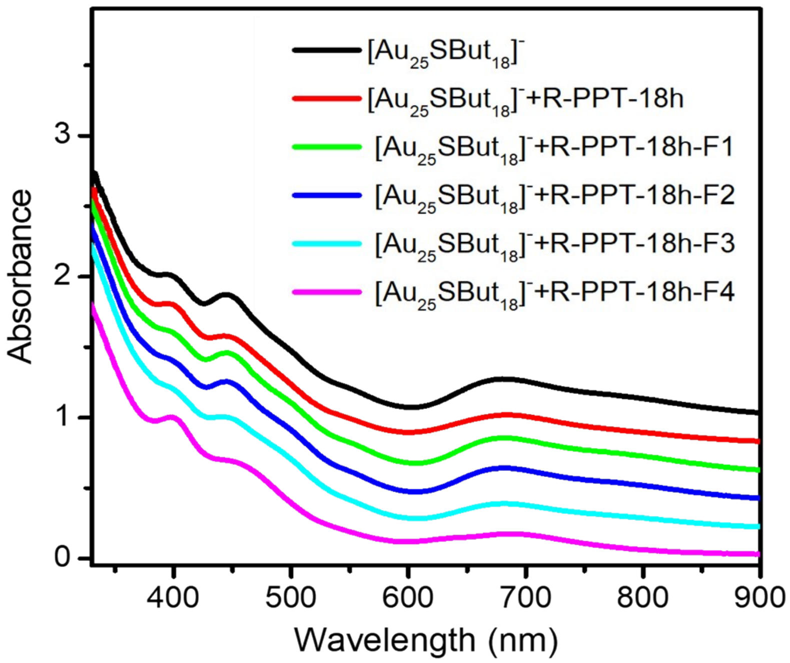

Figure S20. UV-Vis spectra of fractions obtained after LER of 0.1 mM of $[Au_{25}(SBut)_{18}]^-$ with R-PPT at room temperature in dichloromethane. The SBut:R-PPT ratio is 1:2.

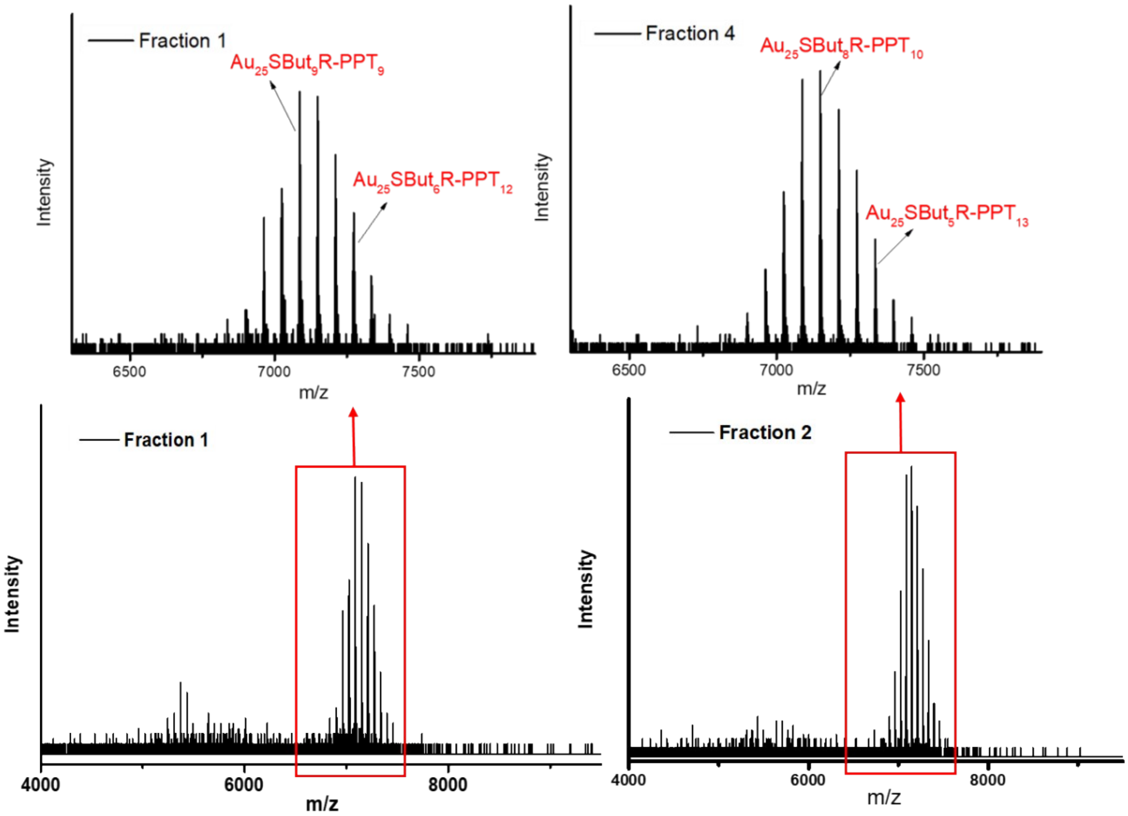

Figure S21. Electrospray ionization (ESI) mass spectroscopy in positive mode of the first and last fractions after LER of 0.1 mM of $[Au_{25}(SBut)_{18}]^-$ with R-PPT at room temperature in dichloromethane.

VI. Circular Dichroism spectroscopy

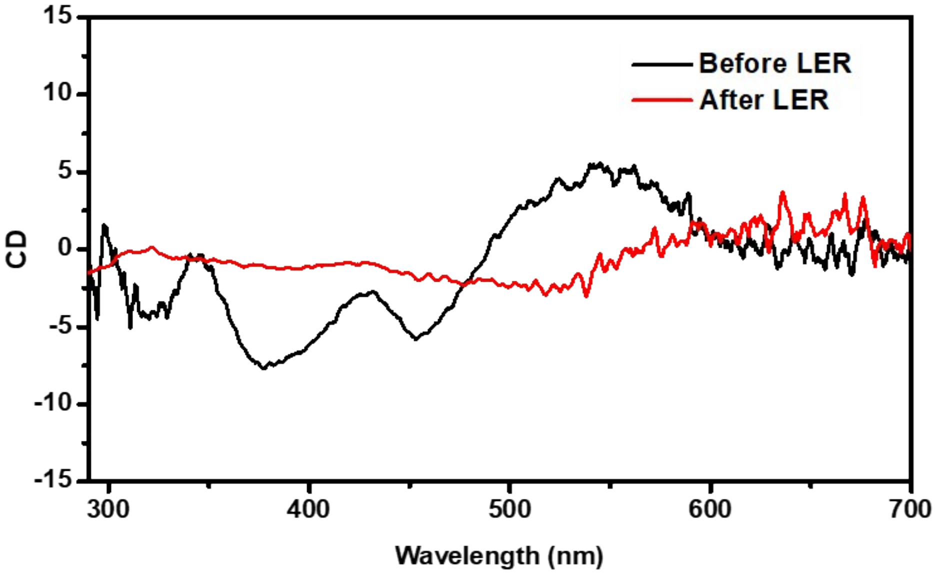

Figure S22. CD spectra of LER between $Au_{28}(S\text{-}PPT)_{21}$ and SBut (Figure S11).

Reference

1. M. Zhu, H. Qian, X. Meng, S. Jin, Z. Wu and R. Jin, *Nano Lett.*, 2011, **11**, 3963-3969.